Title

Liquid vaporization actuated soft structures with active cooling and heat loss control

Journal

Smart Materials and Structures, 30(5)

ISSN

0964-1726

Authors

Lee, Han-Joo

Loh, Kenneth J

Publication Date

2021-05-01

DOI

10.1088/1361-665x/abeefb

Peer reviewed

Liquid Vaporization Actuated Soft Structures with Active Cooling and Heat Loss Control

Han-Joo Lee[1] and Kenneth J. Loh[1,2,*]

[1] Material Science and Engineering Program, University of California San Diego, La Jolla, CA 92093-0418, USA
[2] Department of Structural Engineering, University of California San Diego, La Jolla, CA 92093-0085, USA

[*] Corresponding author e-mail: kenloh@ucsd.edu

Soft robotic systems that are inspired by nature utilize soft materials to perform various tasks in diverse environments. One promising method to control their movement is by utilizing liquid vaporization. In most cases, liquid with high vapor pressure is injected into hollow cavities inside the elastomer. Heating the system vaporizes the liquid, and the structure is inflated by the generated gas. However, there is a significant time lag between powering the system and structural actuation due to the slow increase in temperature that is exacerbated by heat loss. Simply using materials with low thermal conductivity can improve actuation, but the reduced heat loss concurrently increases cooling time during the reversing process. Furthermore, underwater actuation through vaporization remains a challenge, since heat loss becomes even more significant. To address these issues, this study aims to develop a system that can actively control heat loss to enhance both actuation and cooling while performing consistently even in extreme environments. First, double-walled structures were fabricated with silicone elastomer to drastically lower thermal conductivity. Next, a thermoelectric device was installed on the bottom layer to heat and cool the sealed liquid by reversing current flow. The low thermal conductivity of the double-walled structure enhanced actuation performance, while actively cooling the system with the thermoelectric device accelerated the reversing process. Structures with single- and double-layered walls were tested underwater to validate their performance. Finite element models verified the effects of wall designs on heat transfer and structural mechanics. Demonstration of enhanced reversible actuation of the system was performed using a soft anemone-like structure operated underwater.

Keywords: Phase transformation, soft actuation, thermal conductivity, thermoelectric device, vaporization.

Introduction

The bio-inspired soft robotics field focuses on creating innovative soft structures and soft actuation methods that mimic biological motions and materials to perform complex functionalities. Depending on the actuation method, applying the system underwater can be challenging due to the additional pressure and cooling from the surrounding liquid. To date, several different underwater soft material actuators have been demonstrated, including the use of fluidic pumps[1-3], hydrogels[4-7], dielectric elastomers[8-10], ionic polymer-metal composites[11,12], liquid vaporization[13,14], liquid crystal gels[15], shape memory alloys[16], and coiled polymers[17]. While pumps and liquid vaporization rely on pressure applied to the inner walls, other methods utilize materials that deform when subjected to external stimuli.

This study focuses on soft actuation enabled by liquid vaporization, which is a promising method that enables simple and untethered systems. In most cases, the system is composed of a heating source and a soft structure filled with liquid. The liquid with high vapor pressure is heated to boiling by injecting current to an embedded heating element. During phase transformation, the generated gas inflates the soft structure and results in actuation. In general, a very small amount of liquid is required to inflate the structure, since 1 mole of liquid can generate as much as 22.4 L of gas under standard temperature and pressure condition. Increasing the amount of liquid only increases the time to heat and to raise the temperature of the entire system. The amount of power injected into the heating element determines the

temperature of the liquid, which directly affects actuation performance. As compared to inflating the structure by using a pneumatic pump, actuation by vaporization uses small components that can be easily packaged into a miniature system. This makes the method favorable for applications that demand portable or untethered systems.

However, the dominating limitation of vaporization is the speed of actuation, which is limited by the time for heating the liquid to boiling. In addition, a large amount of energy is required to increase the temperature of the liquid and soft elastomer due to their high specific heat capacity. If the heater is installed inside the elastomer, the low thermal conductivity of the material further reduces actuation speed. After actuation, the condensation process is even slower. Whereas actuation can be improved by injecting more current into the joule heating element, the reversing process simply relies on ambient air cooling. Similar to actuation, this cooling process is also slow due to the high specific heat capacity and low thermal conductivity of soft elastomers. Furthermore, actuating structures underwater through vaporization remains a challenge, since the surrounding water act as a heat sink and slows the heating process. Excessive heating is required to achieve considerable temperature increases when the system is operated underwater.

Nevertheless, several techniques have been developed to fully utilize liquid vaporization for soft actuation. A popular method involves installing a joule heating element inside the structure to boil the embedded liquid[18-22]. These studies applied current to conductive wires or fabrics installed inside soft elastomers for joule heating. Ethanol was either filled in hollow chambers or distributed in small cavities inside the elastomer matrix. Oh *et al.*[22], in particular, addressed the slow thermal-response time and installed microcapsules of liquid metal to increase thermal conductivity. Other methods heated the soft structures from external sources such as an oven[23], heated surface[24], or even lasers[25,26]. The benefit of these methods is that the system does not need to carry a power supply and can easily be untethered for deployment. Another recent study installed an atomizer inside the structure to avoid the time lag from heating bulk liquid[27]. The atomizer dispersed the liquid into small droplets, which evaporated immediately as they passed through a heater. Evaporation rapidly actuated the structure even when the temperature was well below boiling.

Despite these various approaches, comparing the performance of these studies are not straightforward, since actuation through vaporization is an intricate process. In most cases, actuation involving heat occurs under non-equilibrium conditions, making it difficult to analyze. Moreover, actuation is also affected by the thermal properties of the liquid and encasing structure. Even when implementing the same heating mechanism, using a liquid with higher vapor pressure will improve actuation. The thermal conductivity of the soft material, as well as the geometry of the structure, also affect heat loss during both the actuation and cooling processes. Furthermore, the effect of heat loss can become even more significant depending on its operational environment (*e.g.*, underwater). As a result, heat transfer analysis is imperative to better understand the actuation mechanism.

This study focused on actively controlling heat loss to enhance speed during both the actuation and cooling processes and to develop a system that can perform consistently in various thermal environments. In general, heat can be lost through conduction, convection, and radiation. While all three mechanisms are worth investigating to fully control heat loss, this study focused on adjusting thermal conductivity by incorporating a layer of air between the walls. Different wall designs were analyzed using finite element (FE) modeling to study how it affects heat transfer and structural mechanics. Tests were conducted on a soft elastomer to determine the parameters necessary for FE modeling of the heat transfer process. Simple cuboid structures with single- and double-layered walls were designed to analyze heat loss, as well as displacement during inflation. When fabricating the structure, soft double-layered walls were combined with a thermoelectric device to manipulate heat loss. During actuation, the thermoelectric layer was powered to heat the system, while the double-layered walls minimized heat loss. After actuation, current flow to the thermoelectric device was reversed, which increased heat dissipation and allowed rapid cooling inside the structure. Testing the structure underwater further enhanced the Peltier effect and increased cooling rate. For validation, a soft anemone-like structure was fabricated and operated underwater, which opened upon actuation and closed during cooling. Its actuation and cooling speeds were compared with different conditions to validate the potency of the method.

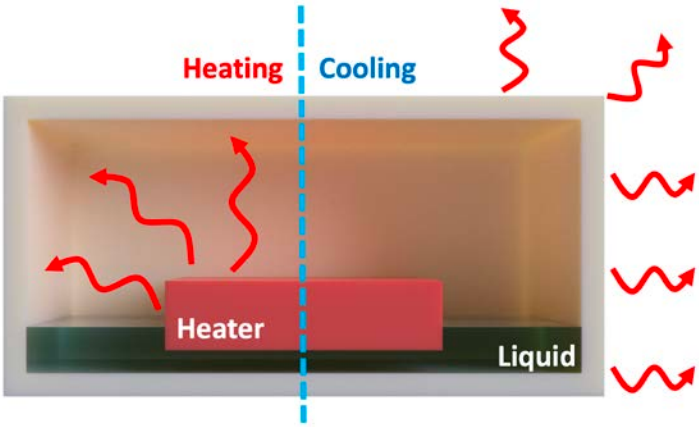

Figure 1. The illustration shows how heat loss affects soft actuation during vaporization and the cooling process.

Materials and Methods

Effect of soft elastomer properties

Thermal properties of soft materials have a substantial influence on reversible actuation through vaporization. Fig. 1 shows a schematic of the actuator system. The cross-section illustrates a soft cuboid structure that is partially filled with liquid; the left half shows the heating (*i.e.*, actuation) process. Temperature is increased to boiling by injecting current into the heater. During this process, the thermal conductivity of the walls should be low enough to effectively contain heat inside the chamber. High thermal conductivity will result in significant heat loss, which in turn slows actuation. On the other hand, the right half of the illustration in Fig. 1 shows the cooling process that returns the structure to its original shape. Since the amount of gas inside the structure is directly dependent on temperature, high heat loss is required to quickly reverse actuation, which can be improved by using materials with high thermal conductivity. These competing requirements mean that systems without a method to actively control heat loss will always sacrifice either actuation or cooling performance.

In this work, the wall design of soft materials was combined with a thermoelectric device to maximize both the forward and reverse actuation performance. Double-layered, versus single-layered, walls were studied to reduce heat loss and to increase displacement during inflation. When fabricating the structure, a commercial thermoelectric device was used as the bottom layer. Thermoelectric devices are operated to induce a temperature difference between its opposite surfaces, which was used to heat and cool the liquid inside the chamber by reversing current flow. Since Peltier cooling performs best when there is a heatsink on the heated side, the system showed high potential when used underwater. While the low thermal conductivity of the double-walled structure improves actuation, the thermoelectric device can improve the reversing (*i.e.*, cooling) process. Recent advancements in thermoelectric systems, such as flexible thermoelectric devices[28], enable realization of a fully soft heating and cooling system.

Soft material characterization

Dragon skin FX-Pro was used as the soft elastomer in this study. The thermal conductivity and heat capacity of Dragon skin was measured through simple experiments. A hot wire method was used to measure thermal conductivity, which is illustrated in Fig. 2(a)[29-31]. A Nichrome wire was installed through the middle of a cylindrical Dragon skin structure. While heating the structure, temperature was recorded with a thermocouple embedded inside the material. The thermal conductivity, λ, was calculated by:

$$\lambda = \left(\frac{q}{4\pi}\right) \cdot \left(\frac{dT}{d(\ln \tau)}\right)^{-1} \quad (1)$$

where q is specific heat output, T is temperature, and τ is time. The measured temperature can be plotted as a function of logarithmic time, and equation (1) becomes:

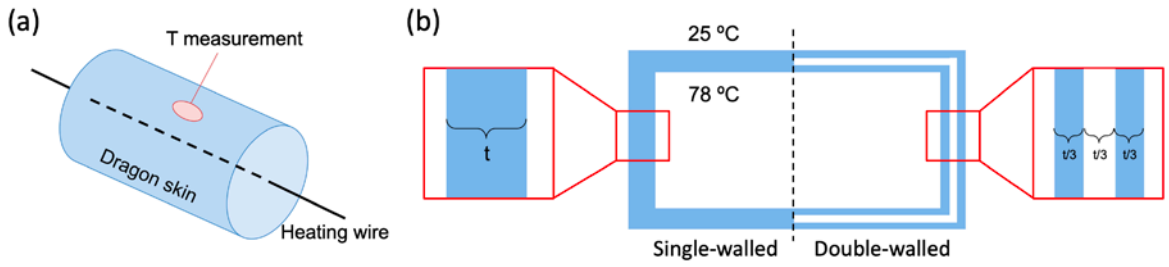

Figure 2. (a) A hot wire method was used to measure the thermal conductivity of the soft Dragon skin. (b) The illustration shows how the walls were designed for FE modeling. The temperature of the inside and outside of the chamber was 78 °C and 25 °C, respectively.

$$\lambda = \frac{Ri^2}{l4\pi a} \tag{2}$$

where R is resistance, i is current, l is length of Dragon skin, and a is the slope. The measured thermal conductivity of Dragon skin was ~ 0.25 W/mK.

Finite element modeling

Two FE modeling studies were conducted with COMSOL to analyze heat transfer and structural mechanics. Since actuation involves numerous physics (*i.e.*, joule heating, Peltier effect, heat transfer, phase transformation, and structural mechanics), the two simulations were simplified to decrease computation time and analyze how the double-walled design directly affects heat loss and inflation individually. The cross-section of the designed structure is shown in Fig. 2(b). The left half shows a single-walled structure, whereas the right half shows a double-walled structure. The double-walled structure had three layers of material (*i.e.*, Dragon skin, air, and Dragon skin), and the total thickness, t, was equivalent to the single-layer. Heat loss analysis was conducted by assuming that the temperature inside the structure was 78 °C, which is the boiling temperature of ethanol (*i.e.*, the embedded fluid). In addition, the surrounding temperature was assumed to be 25 °C, since the fabricated structure was tested underwater. The total amount of heat loss was simulated by assuming the temperature of the surrounding and inside the chamber are constant. Structural mechanics was also used to determine how the walls affect displacement during inflation through a separate study. The Neo-Hookean model was used to define the hyperelastic material, with its shear modulus (64.7 kPa) obtained from a previous study[32]. The bottom layers were assumed to be fixed in place, while the ideal gas law was used to define the gas inside the chamber and the layer in between two elastomer walls. The pressure inside the chamber, as well as the air layer between the double-layered wall, were updated using:

$$\frac{P}{P_0} = \left(\frac{V_0}{V}\right)^{\gamma} \tag{3}$$

where P is pressure, V is volume, and γ is specific heat ratio, and subscript 0 denotes the initial condition. The maximum displacement of the top layer was measured when the initial pressure of ~ 1.2 atm (equivalent to the vapor pressure of ethanol at ~ 45 °C) was applied to the inner wall.

Fabrication

In this study, 3D-printed polylactic acid (PLA) rigid molds were used to fabricate the soft structures. Two parts of Dragon skin (Part A and Part B) were hand-mixed at a 1:1 weight ratio, and the mixture was placed in a vacuum chamber before pouring it into the mold. The mold was then placed in the vacuum chamber one more time to remove any bubbles formed during pouring. Then, the mold was left at room temperature for ~ 1 h to fully cure the silicone elastomer. Fig. 3(a) shows the cross-section of the cuboid actuator. Next, the thermoelectric device was placed at the bottom opening of the cuboid structure, and uncured Dragon skin was applied to seal the gap. A syringe was used to inject 2 mL of ethanol into the chamber, and the hole was sealed with the same elastomer in a similar way. The size

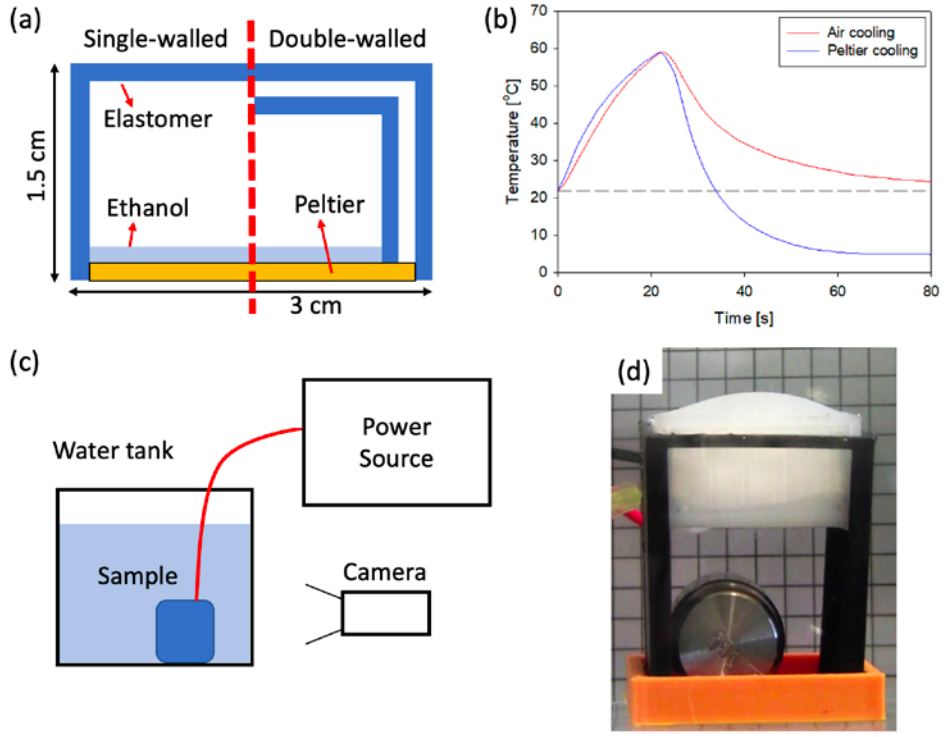

Figure 3. (a) The cross-section shows the design of the fabricated single- and double-walled soft structure. (b) The performance of the thermoelectric device is shown, where the temperature of the inner surface was measured. The inner surface reached ~ 60 °C after 20 s of heating. The system was then cooled by both air cooling and Peltier cooling. (c) The schematic shows the experimental setup. (d) The structure was actuated underwater to measure displacement over time.

of the single-layered structure (3 cm × 3 cm × 1.5 cm) was fabricated with 1 mm thick walls. After testing, a slightly smaller cuboid structure with 1 mm thickness was installed on the inside to form the double-walled structure.

The performance of the thermoelectric Peltier device is plotted in Fig. 3(b). An open-ended structure without ethanol was positioned so that the bottom (*i.e.*, outer) layer was in contact with water, while the top (*i.e.*, inner) layer was exposed to air. The amount of current was selected by slowly increasing the voltage until steady cooling was maintained on the top layer without excessive joule heating. The maximum voltage of 2.5 V resulted in ~ 1 A of current. During the first phase, current was injected so that the top layer heated while cooling the bottom layer. After heating, current flow was reversed to cool the top layer while heating the bottom layer. Temperature change during heating and air cooling is plotted in red in Fig. 3(b), whereas the blue plot shows temperature change during heating and Peltier cooling. The temperature reached ~ 60 °C after ~ 20 s of heating and decreased much faster during Peltier cooling as compared to air cooling. The temperature reached 25 °C after ~ 50 s when air cooled, whereas Peltier cooling decreased the cooling time by ~ 80%, taking only ~ 10 s.

The setup of the underwater test is shown in Fig. 3(c), where the sample was placed in a large tank of water (30 cm × 17 cm × 22 cm). The Peltier device was connected to a power source, and the actuation was recorded by a camera. Fig. 3(d) shows an image of the sample inside the tank, where a grid with 5 mm spacing was placed in the background. A fixture was 3D-printed with PLA to hold the soft structure. A platform was designed underneath the structure to place weights to prevent the system from floating due to buoyancy. Soft actuation was recorded by video during heating and cooling, and the displacement of the top layer was analyzed by post-processing individual image frames.

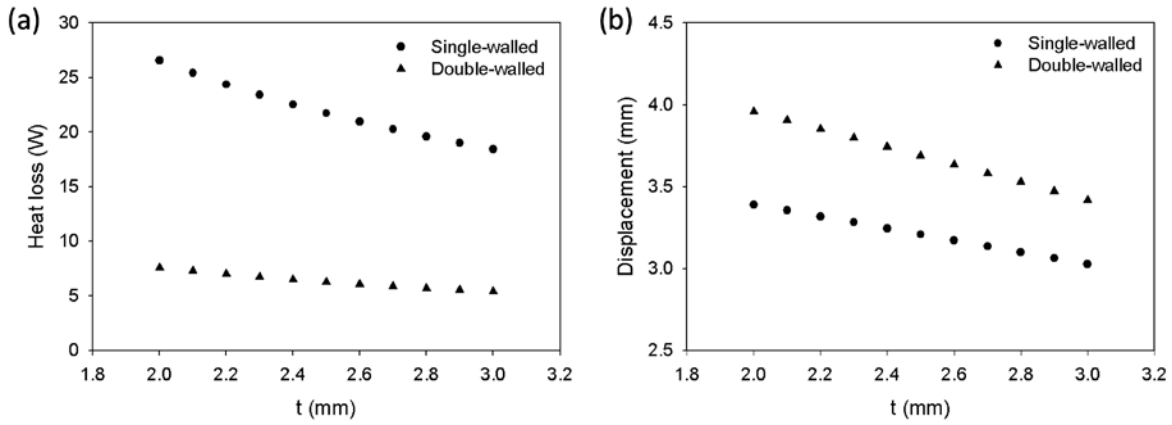

Figure 4. (a) An FE model was used to analyze the heat loss of single- and double-walled structures over a range of total wall thicknesses. (b) The displacement of the top layer was analyzed when the structures were inflated.

Results and Discussion

FE modeling results

The heat loss results are plotted in Fig. 4(a). When *t* was 2 mm, the heat loss of single- and double-walled structures were ~ 27 W and ~ 8 W, respectively. This value decreased rapidly as *t* increased for the single-walled structure and reached ~ 18 W when *t* was 3 mm. On the other hand, the double-walled structure showed very small changes with increasing thickness. From the results, it is evident that simply adding a thin layer of air drastically decreased system heat loss. Overall, heat loss from the single-walled structure was ~ 3.5 times higher than the double-walled one. Similarly, the displacement of the top layer during inflation is plotted in Fig. 4(b). When *t* was 2 mm, the displacement of the single- and double-walled structure was ~ 3.4 mm and ~ 4 mm, respectively. With increasing *t*, these values declined at a similar rate (or slope). Although the difference was not significant, the displacement of the single-walled structure was ~ 1.2 times higher than the double-walled structure. The results show that fabricating the structure with double-layered walls would enhance the actuation phase due to low heat loss while attaining higher displacement under the same conditions. Although these simplified simulations do not represent the exact values of the following experiment, the results show a straightforward insight on how the double-layered wall design affects heat loss and displacement in general.

Actuation and active cooling

Fig. 5 shows the displacement results when actuating the fabricated structure. Each structure was tested in two different environments. During the first test, the structure was fixed in place above water so that only the bottom layer of the

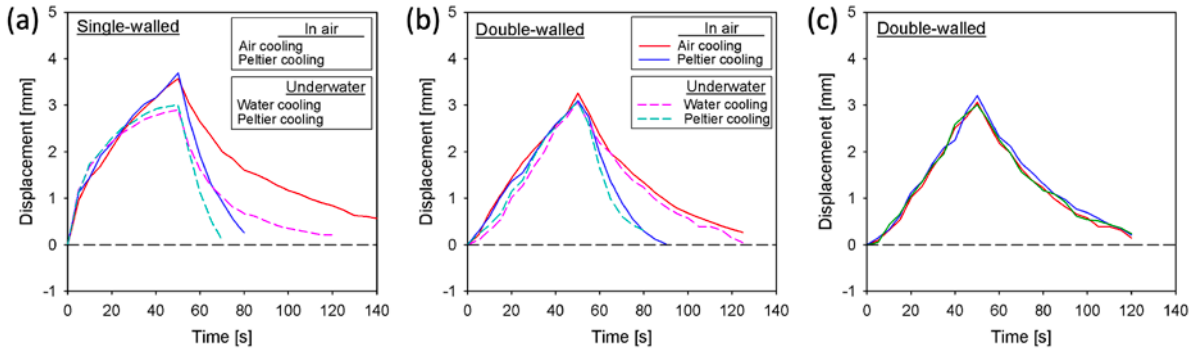

Figure 5. (a) The single-walled structure was actuated in air and underwater. The structure was actuated for 50 s and cooled down by either turning off the device or reversing the current for Peltier cooling. (b) The double-walled structure was tested under the same conditions. (c) The double-walled structure was actuated and cooled underwater 3 times to show consistency.

Peltier device was in contact with liquid. This allowed maximum cooling from the device, while the soft walls were exposed to air. Afterwards, the entire structure was submerged underwater. For each environment, the structure was actuated by heating the thermoelectric device for ~ 50 s, followed by cooling the system to return to its original shape. The system was cooled by simply turning off the thermoelectric device (*i.e.*, for air or water cooling) or reversing current for active Peltier cooling. The displacements were used to represent the performance of the actuation and reversing processes.

The single-walled structure had a wall thickness of 1 mm, and the results are shown in Fig. 5(a). The solid lines show the results for the structure that was exposed to air, whereas the dashed lines are results for the submerged structure. The structure reached a displacement of ~ 3.5 mm when in air, while it achieved ~ 3.0 mm of displacement underwater. The actuation rate decreased faster when the structure was underwater and began to plateau. This was due to the large heat loss from the single-walled structure, and it can be assumed that displacement will stabilize even upon further heating when the system reaches thermal equilibrium. After actuation, displacement decreased slowly once power was shut off. In contrast, when current was reversed for Peltier cooling, the displacement decreased at a much faster rate. To compare the cooling rates, the time it took for displacement to return to 0.5 mm was analyzed for both methods. When the single-walled structure was exposed to air, Peltier cooling reduced cooling time by ~ 74% with respect to air cooling. When submerged underwater, actively cooling the system with the thermoelectric device reduced cooling time by ~ 62% as compared to water cooling.

The same set of tests was conducted after adding an additional 1 mm thick layer within the previous structure to form the double-walled system, and the results are plotted in Fig. 5(b). As compared to the previous single-walled structure, the tests conducted in air and underwater showed little difference. This indicates that the double-walled structure was not significantly affected by its environment due to very low thermal conductivity. Although the increase in displacement during actuation was smaller due to the additional layer and greater structural stiffness, the slope was fairly linear and consistent even after 50 s of actuation. Unlike the single-walled structure, continued heating was expected to further increase its displacement. During cooling, Peltier cooling decreased cooling time by ~ 60% versus simply turning off power for air cooling. The double-walled structure was actuated and actively cooled three times, and the results are plotted in Fig. 5(c). The overlaid results show that the method performed consistently and was repeatable.

These results show several benefits of combining thermoelectric devices with double-walled structures that are actuated underwater. First, the low thermal conductivity of the soft walls enhances actuation by reducing heat loss. When heat dissipation is significant, the system quickly reaches thermal equilibrium, where the input power is the same as heat loss. Second, change in environment has little effect on actuation performance. This is especially important when the system is deployed in unpredictable situations. Last, the thermoelectric device can effectively improve the cooling process. While fabricating the entire structure with double-layered walls can improve actuation, water cooling will take longer due to its low thermal conductivity. This can be resolved by actively cooling the system with a thermoelectric device.

Anemone demonstration

A soft Dragon skin FX-Pro structure in the form of an anemone was fabricated to mimic its movements and to validate rapid actuation. Anemones in nature use their muscles to open/close its tentacles[33], burrow in sand[34], and even swim[35]. These delicate and complex movements are difficult to imitate with conventional rigid robotics. In this study, the opening and closing motions of the mouth and tentacles were demonstrated by inflating the soft structure. Fig. 6(a) shows a 3D-printed PLA mold used to fabricate the top tentacle layer. First, uncured Dragon skin was left at room temperature for ~ 15 min until it became viscous. Then, the mold was dipped in the mixture to create a uniform layer around its surface. A heat gun was used to rapidly cure the elastomer, and the process was repeated twice to fabricate a durable layer. Finally, the elastomer was stretched and peeled off the mold.

The cross-section of the anemone structure is shown in Fig. 6(b). A separate hollow cylindrical structure was fabricated and sealed with the tentacle layer on top. Similar to the cuboid structure, both single-walled and double-walled artificial anemone structures were fabricated for comparison. The same thermoelectric device was installed at the bottom layer, and 2 mL of ethanol was injected into the chamber.

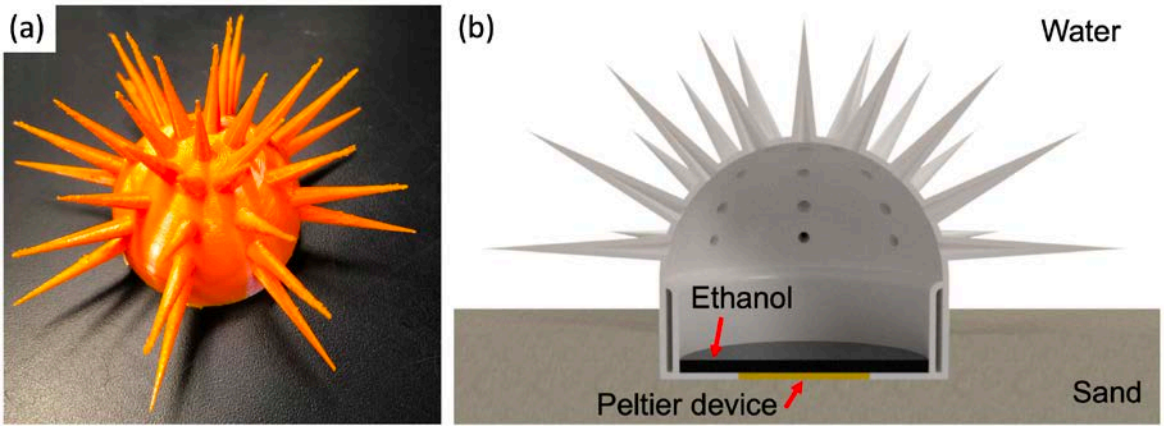

Figure 6. (a) A mold was 3D-printed to fabricate the top tentacle layer of the artificial anemone. (b) The illustration shows the cross-section of the fabricated double-walled anemone, which was partially burrowed in sand underwater.

Fig. 7 shows the anemone structure that was partially burrowed into the sand underwater. Since the sand was also wet, it still functioned as a proper heat sink. Here, 5 V was applied to the system during actuation to heat the embedded ethanol. The applied voltage effectively heated the structure through a combination of Peltier effect and joule heating. After actuation, the device was either turned off for water cooling, or current was reversed for active Peltier cooling. While cooling the structure with the thermoelectric device, voltage was reduced to 2.5 V to prevent excessive joule heating. When actuating the single-walled structure, inflation slowed and stopped before full deployment. This was consistent with the previous test, where the displacement change of the cuboid structure slowed down due to greater heat loss. On the other hand, the double-walled structure fully inflated until the tentacle layer was completely actuated after ~ 60 s. During cooling, Peltier cooling was significantly more effective while reducing cooling time by ~ 55% versus ambient water cooling. Overall, the results confirmed the viability of the proposed actuation and cooling method for soft robotic structures underwater.

Conclusions

This article addresses the importance of thermal conductivity when actuating soft structures through liquid vaporization, while demonstrating a method that improved both the actuation and cooling processes underwater. In underwater environments, heat loss has a significant effect on actuation by phase transformation. While this can be solved by fabricating double-layered walls, the low thermal conductivity will also slow down the cooling process. In

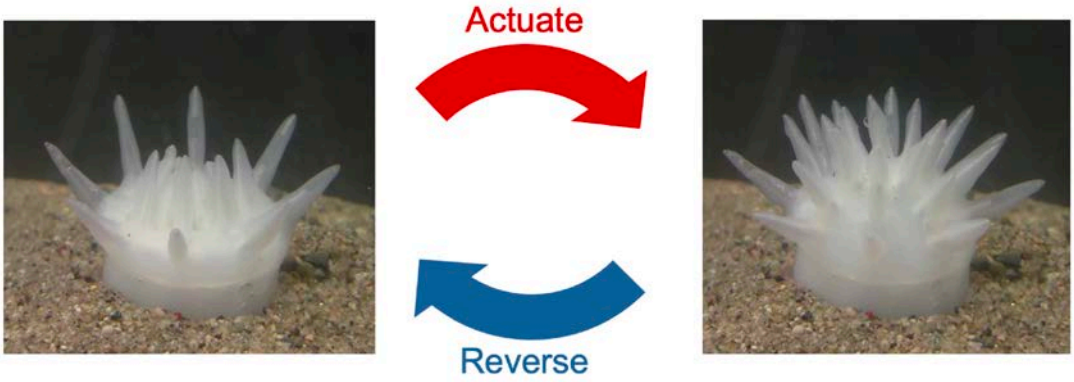

Figure 7. The artificial anemone structure was actuated and cooled to mimic the opening and closing motion of its biological counterpart.

order to improve the reverse actuation process, a thermoelectric device was used to actively cool the system. FE modeling results showed how the double-walled structure reduced heat loss while simultaneously increasing the displacement during inflation when the wall thicknesses were kept the same. When testing the fabricated structures, the thermoelectric device was used to heat and cool the system. The actuation speed of the single-walled structure underwater decreased rapidly due to significant heat loss. On the other hand, the double-walled structure showed more stable actuation, and cooling down the system by Peltier cooling reduced the required time to less than half as compared to water cooling. This was achieved by simply reversing current flow, and the method does not require an additional power source for cooling. While most studies implement fluidic pumps for underwater applications that require precise and rapid movements, they must encase a large and heavy pump that is tethered to the chamber. Although slower, actuation through vaporization only requires a small heater that is connected to a power source. The proposed method opens new possibilities to apply actuation through vaporization in unpredictable or harsh surroundings, especially underwater, where the liquid significantly hinders the heating process.

Acknowledgements

This research was supported by the U.S. National Science Foundation under grant numbers CMMI-1762530 and CMMI-2032021. Additional support was provided by the Jacobs School of Engineering, University of California San Diego. The authors acknowledge the collaboration of Prof. Hyunsun Kim at the University of California San Diego.

References

1. Marchese, A. D., Onal, C. D. & Rus, D. Autonomous soft robotic fish capable of escape maneuvers using fluidic elastomer actuators. *Soft Robotics* **1**, 75-87, (2014).
2. Shen, Z., Zhong, H., Xu, E. C., Zhang, R. Z., Yip, K. C., Chan, L. L., Chan, L. L., Pan, J., Wang, W. P. & Wang, Z. An underwater robotic manipulator with soft bladders and compact depth-independent actuation. *Soft Robotics* **7**, 535-549, (2020).
3. Kurumaya, S., Phillips, B. T., Becker, K. P., Rosen, M. H., Gruber, D. F., Galloway, K. C., Suzumori, K. & Wood, R. J. A modular soft robotic wrist for underwater manipulation. *Soft Robotics* **5**, 399-409, (2018).
4. Li, T. F., Li, G. R., Liang, Y. M., Cheng, T. Y., Dai, J., Yang, X. X., Liu, B. Y., Zeng, Z. D., Huang, Z. L., Luo, Y. W., Xie, T. & Yang, W. Fast-moving soft electronic fish. *Science Advances* **3**, e1602045, (2017).
5. Migliorini, L., Santaniello, T., Yan, Y. S., Lenardi, C. & Milani, P. Low-voltage electrically driven homeostatic hydrogel-based actuators for underwater soft robotics. *Sensors and Actuators B-Chemical* **228**, 758-766, (2016).
6. Santaniello, T., Migliorini, L., Locatelli, E., Monaco, I., Yan, Y. S., Lenardi, C., Franchini, M. C. & Milani, P. Hybrid nanocomposites based on electroactive hydrogels and cellulose nanocrystals for high-sensitivity electro-mechanical underwater actuation. *Smart Materials and Structures* **26**, 085030, (2017).
7. Cheng, Y., Huang, C., Yang, D., Ren, K. & Wei, J. Bilayer hydrogel mixed composites that respond to multiple stimuli for environmental sensing and underwater actuation. *Journal of Materials Chemistry B* **6**, 8170-8179, (2018).
8. Christianson, C., Goldberg, N. N., Deheyn, D. D., Cai, S. Q. & Tolley, M. T. Translucent soft robots driven by frameless fluid electrode dielectric elastomer actuators. *Science Robotics* **3**, eaat1893, (2018).
9. Shintake, J., Cacucciolo, V., Shea, H. & Floreano, D. Soft biomimetic fish robot made of dielectric elastomer actuators. *Soft Robotics* **5**, 466-474, (2018).
10. Berlinger, F., Duduta, M., Gloria, H., Clarke, D., Nagpal, R. & Wood, R. A modular dielectric elastomer actuator to drive miniature autonomous underwater vehicles. *2018 Ieee International Conference on Robotics and Automation (Icra)*, 3429-3435, (2018).
11. Shen, Q., Olsen, Z., Stalbaum, T., Trabia, S., Lee, J., Hunt, R., Kim, K., Kim, J. & Oh, I. K. Basic design of a biomimetic underwater soft robot with switchable swimming modes and programmable artificial muscles. *Smart Materials and Structures* **29**, 035038, (2020).
12. Anton, M., Chen, Z., Kruusmaa, M. & Tan, X. B. Analytical and computational modeling of robotic fish propelled by soft actuation material-based active joints. *2009 Ieee-Rsj International Conference on Intelligent Robots and Systems*, 2126-2131, (2009).
13. Li, J. F., Sun, M. J. & Wu, Z. Q. Design and fabrication of a low-cost silicone and water-based soft actuator with a high load-to-weight ratio. *Soft Robotics*, (2020). DOI: 10.1089/soro.2019.0186

14. Kang, B., Lee, Y., Piao, T., Ding, Z. & Wang, W. Robotic soft swim bladder using liquid-vapor phase transition. *Materials Horizons*, (2021). DOI: 10.1039/d0mh01788d
15. Shahsavan, H., Aghakhani, A., Zeng, H., Guo, Y. B., Davidson, Z. S., Priimagi, A. & Sitti, M. Bioinspired underwater locomotion of light-driven liquid crystal gels. *Proceedings of the National Academy of Sciences of the United States of America* **117**, 5125-5133, (2020).
16. Cianchetti, M., Licofonte, A., Follador, M., Rogai, F. & Laschi, C. Bioinspired soft actuation system using shape memory alloys. *Actuators* **3**, 226-244, (2014).
17. Hamidi, A., Almubarak, Y., Rupawat, Y. M., Warren, J. & Tadesse, Y. Poly-saora robotic jellyfish: Swimming underwater by twisted and coiled polymer actuators. *Smart Materials and Structures* **29**, 045039, (2020).
18. Cartolano, M., Xia, B. X., Miriyev, A. & Lipson, H. Conductive fabric heaters for heat-activated soft actuators. *Actuators* **8**, 9, (2019).
19. Oh, S., Kim, S. U., Yeom, S., Kim, H., Kim, S. & Na, J. H. Continuum soft actuators based on reprogrammable geometric constraints. *Extreme Mechanics Letters* **36**, 100649, (2020).
20. Chellattoan, R., Yudhanto, A. & Lubineau, G. Low-voltage-driven large-amplitude soft actuators based on phase transition. *Soft Robotics*, (2020). DOI: 10.1089/soro.2019.0150
21. Li, X. Y., Duan, H. L., Lv, P. Y. & Yi, X. Soft actuators based on liquid-vapor phase change composites. *Soft Robotics*, (2020). DOI: 10.1089/soro.2020.0018
22. Oh, B., Park, Y. G., Jung, H., Ji, S., Cheong, W. H., Cheon, J., Lee, W. & Park, J. U. Untethered soft robotics with fully integrated wireless sensing and actuating systems for somatosensory and respiratory functions. *Soft Robotics* **7**, 564-573, (2020).
23. Kim, Y. I., An, S., Yarin, A. L. & Yoon, S. S. Performance enhancement of soft nanotextured thermopneumatic actuator by incorporating silver nanowires into elastomer body. *Soft Robotics*, (2020). DOI: 10.1089/soro.2020.0044
24. Nishikawa, Y. & Matsumoto, M. A design of fully soft robot actuated by gas-liquid phase change. *Advanced Robotics* **33**, 567-575, (2019).
25. Han, J., Jiang, W., Niu, D., Li, Y., Zhang, Y., Lei, B., Liu, H., Shi, Y., Chen, B., Yin, L., Liu, X., Peng, D. & Lu, B. Untethered soft actuators by liquid–vapor phase transition: Remote and programmable actuation. *Advanced Intelligent Systems* **1**, 1900109, (2019).
26. Hiraki, T., Nakahara, K., Narumi, K., Niiyama, R., Kida, N., Takamura, N., Okamoto, H. & Kawahara, Y. Laser pouch motors: Selective and wireless activation of soft actuators by laser-powered liquid-to-gas phase change. *Ieee Robotics and Automation Letters* **5**, 4180-4187, (2020).
27. Lee, H.-J., Prachaseree, P. & Loh, K. J. Rapid soft material actuation through droplet evaporation. *Soft Robotics*, (2020). DOI: 10.1089/soro.2020.0055
28. Hong, S., Gu, Y., Seo, J. K., Wang, J., Liu, P., Meng, Y. S., Xu, S. & Chen, R. K. Wearable thermoelectrics for personalized thermoregulation. *Science Advances* **5**, eaaw0536, (2019).
29. dos Santos, W. N. & Gregorio, R. Hot-wire parallel technique: A new method for simultaneous determination of thermal properties of polymers. *Journal of Applied Polymer Science* **85**, 1779-1786, (2002).
30. Healy, J. J., Degroot, J. J. & Kestin, J. Theory of transient hot-wire method for measuring thermal-conductivity. *Physica B & C* **82**, 392-408, (1976).
31. Merckx, B., Dudoignon, P., Garnier, J. P. & Marchand, D. Simplified transient hot-wire method for effective thermal conductivity measurement in geo materials: Microstructure and saturation effect. *Advances in Civil Engineering* **2012**, 625395, (2012).
32. Lee, H.-J., Melchor, N., Chung, H. & Loh, K. J. Characterization of a soft gripper with detachable fingers through rapid evaporation. *2020 3rd IEEE International Conference on Soft Robotics (RoboSoft)*, 83-88, (2020).
33. Batham, E. J. & Pantin, C. F. A. Muscular and hydrostatic action in the sea-anemone metridium-senile (l). *Journal of Experimental Biology* **27**, 264-289, (1950).
34. Ansell, A. D. & Trueman, E. R. The mechanism of burrowing in the anemone, peachia hastata gosse. *Journal of Experimental Marine Biology and Ecology* **2**, 124-134, (1968).
35. Sund, P. N. A study of the muscular anatomy and swimming behaviour of the sea anemone, stomphia-coccinea. *Quarterly Journal of Microscopical Science* **99**, 401-420, (1958).